Catalysis Science & Technology

Accepted Manuscript

ROYAL SOCIETY OF CHEMISTRY

www.rsc.org/catalysis

Cu, Al and Ga based metal organic framework catalysts for the decarboxylation of oleic acid

L. Yang, G. L. Ruess, M.A. Carreon*

Keywords: metal organic frameworks,decarboxylation, fuel hydrocarbons

Abstract

Herein we demonstrate the catalytic decarboxylation and conversion of oleic acid to paraffins, and hydrocarbons over bare and Pt supported Cu, Al and Ga based metal organic frameworks. Moderate degree of decarboxylation were observed for all metal organic framework catalysts. The incorporation of Pt with the porous frameworks resulted in high degrees of decarboxylation. All MOF catalysts showed high thermal stability, resulting in recyclable catalysts displaying low catalytic activity loss. Of all studied catalysts, Ga-MOF catalysts were the most effective catalysts, displaying moderate to high degrees of decarboxylation. In addition, the Pt-Ga-MOF catalyst displayed selectivity to heptadecane, an important industrial chemical. Octadecane, heptadecane, dodecane, undecane, decane, nonane, octane, heptane were observed as the main side products. To our best knowledge, the catalytic ability of a metal organic framework both as catalyst and support for the decarboxylation of a model fatty acid molecule is reported for the first time.

1. Introduction

The removal of oxygen from fatty acids (deoxygenation) leads to the formation of paraffinic hydrocarbons that can potentially serve as or be converted to direct replacements for traditional petroleum-derived liquid transportation fuelsand paraffinic petrochemical feedstocks [1].Typically, the deoxygenation of unsaturated fatty acids is accomplished via hydrogenation of double bonds and further removal of the carboxyl group by releasing carbon dioxide and producing a paraffinic hydrocarbon, process known as decarboxylationor by releasing carbon monoxide and producing an olefinic hydrocarbon, process known as decarbonylation [2-5].

Considerable studies on liquid phase deoxygenation of free fatty acids and fatty acid esters have been carried out [4-16]. Different metals including Ni, Ni/Mo, Ru, Pd, Pd/Pt, Pt, Ir, Os and Rh impregnated on different supports have been evaluated for their deoxygenation performance under elevated temperatures and pressures.

Several studies of the decarboxylation of the unsaturated oleic acid have been documented [5, 17-31]. Representative examples include Pt-Re/C [21] , Pt/C [21, 25] , Pd/C [22,23,25] ,Molybdenum nitrate, Tungsten nitride and Vanadium nitride supported on γ-Al_2O_3 [24] , Pt/SiO_2 [25], hydrotalcite [26] , Ni/MgO-Al_2O_3 [27] , H_3PO_4/Al_2O_3 [28], Ru/CeO_2 [16] or Pt/CeO_2 [29], natural aluminosilicate as well as nano-sized titanium and magnesium oxide [30]. In most of these reports, the support is catalytically inert material like carbon or relatively, non-acidic components, like silica or non-acidic alumina. Recently, our group has reported the catalytic decarboxylation and conversion of oleic acid to branched and aromatic hydrocarbons in a single process step, over acidic and basic supports including Pt–SAPO-11 and Pt/chloride Al_2O_3 [32] and Pt/SAPO-34, Pt/DNL-6, Pt/RHO and Pt/hydrotalcite [33].

Metal organic frameworks (MOFs) [34,35] have emerged as an appealing type of crystalline microporous materials which combine highly desirable properties, such as uniform micropores, high surface areas, and exceptional thermal and chemical stability, making them ideal candidates for catalytic applications. MOFs consist of metal cations or metal-based-clusters linked by organic molecules forming a crystalline network, which after removal of guest species may result in three dimensional structures with permanent porosity. [34,36,37] Although the catalytic ability of several MOF compositions has been demonstrated for diverse relevant chemical reactions [38,39] to our best knowledge the catalytic performance of MOFs for the decarboxylation of fatty acid molecules has not been reported.

Herein, we report the catalytic decarboxylation of oleic acid to paraffins, and hydrocarbons over isostructural MOFs composed of Cu, Al and Ga catalysts of different acidity. Interestingly, all MOFs displayed moderate catalytic activity even in the absence of Pt. Of all studied catalysts, Ga-MOF catalysts were the most effective catalysts, displaying moderate to high degrees of decarboxylation. Furthermore, the Pt-Ga-MOF catalyst displayed selectivity to the linear paraffin heptadecane, a highly valuable industrial product.

2. Experimental

2.1 Catalyst synthesis and characterization:

MOFs were prepared via conventional solvothermal approach [40]. The employed inorganic sources were copper nitrate hemi-pentahydrate (Alfa Aesar, 98%), aluminum isopropoxide (Sigma-Aldrich, ≥99.99%) and gallium nitrate hydrate (Alfa Aesar, 99.9%). The employed organic linker was 1,3,5-benzenetricarboxylic acid (Alfa Aesar, 98%). The molar ratio of inorganic source to linker was kept constant at 1.36:1. In a typical synthesis, 0.6 g of the inorganic metal source were dissolved in 15 mL of deionized water, and 0.4 g of linker were dissolved in 7.5 mL of deionized water and 7.5 mL of ethanol. The mixture was stirred thoroughly for 2 h. The resultant solution was transferred into a 45 mL teflon-lined stainless steel autoclave and heated at different temperatures and times (depending on the inorganic source). For Cu-MOF, the solvothermal temperature was 120ºC and the synthesis time 18 h. For Al-MOF and Ga-MOF, the solvothermal temperature was 180ºC and the synthesis time 24 h. After this time, the autoclave was cooled down to room temperature, and the resultant crystals on the bottom of the autoclave were washed with methanol for 3 times. The crystals were dried overnight in the oven at 80ºC. These three isostructural MOF compositions were chosen based on the different degree of acidities of the metal species (Gallium as hard acid metal and the most acidic and Cu a borderline acid metal and the less acidic).

The three MOFs were impregnated with tetraamine Pt nitrate at 5 %wt. In a typical impregnation step a stoichiometric amount of the Pt source was dissolved in deionized water and then impregnated on 1.8 g of theMOF meanwhile the suspension was stirred. The mixture was dried overnight at 100°C. After that the mixture was calcined at 300°C for 5 h to remove the ligands of the precursor.

The catalysts were characterized by X-ray diffraction (XRD), field emission scanning electron microscopy (FESEM) and thermal gravimetric analysis (TGA). XRD patterns were collected on a Kristalloflex 800 by Siemens at 25 mA and 30 kV with Cu Kα radiation. FESEM images were taken on JEOL ISM-7000F using a field emission gun and an accelerating voltage of 200 kV. TGA profiles were obtained on TGA Q50 under the constant flow of nitrogen.

2.2 Reaction procedure:

Oleic acid (99%, Alfa Aesar) was employed as the model unsaturated fatty acid molecule. Prior to the catalytic tests, all the catalysts were pre-activated in oven for 3 h at 150ºC. The reactions were conducted in a 100 mL stainless steel, high pressure batch reactor (Parr model 4560). Oleic acid and the catalyst were loaded into the reactor in a mass ratio of 18:1. Before the reaction started, the air in the reactor was removed by flushing hydrogen. After that, the pressure was increased to the desired value (usually 20 bar). Then the reactor was heated to the reaction temperature (320ºC) under constant stirring rate and the temperature was kept constant during the 2 hour reaction period. After the reaction, the catalyst was separated by centrifugation from the product and washed with acetone and hexane for further use. Reaction conditions were chosen based on our previous experience in the decarboxylation of fatty acids [34,35] to optimize the yield of hydrocarbons.

2.3 Product analysis:

The liquid product was collected after reaction and analyzed with a gas chromatograph (GC, 6980N) equipped with a HP-5 MS column (with dimensions of 30 m × 250 µm × 0.25 µm) and a 5973N MSD detector. Before the GC analysis, samples were silylated with N,O-bis(trimethyl)-trifloroacetamide, BSTFA (Sigma-Aldrich, ≥ 99.0%) and kept at 60ºC for 1 h. After that, a sample of 0.2 µL was injected into the GC column (250 ºC, 10.52 psi) with a split ratio 100:1. The carrier gas was helium and the flow rate was 1.0 mL/min. The following GC temperature program was used for analysis: 100ºC for 5 min, 300ºC (1ºC/min for 2 min). The product identification was confirmed with a gas chromatograph-mass spectrometer (GC-MS).

The decarboxylation conversion of the oleic acid was estimated from the reduction in the number of oleic acid carboxylic acid groups during the reaction. The amount of carboxylic acid groups remaining in the products after the reaction was evaluated by quantifying the acid number (ASTMD974). Acid number is the mass of potassium hydroxide (KOH) in milligrams that is required to neutralize one gram of chemical substance.

To quantify the acid number, a known amount of sample (0.1g) was dissolved in a solvent (ethanol + Petroleum ether), then titrated with a solution of sodium hydroxide (NaOH, 0.1N) using phenolphthalein as a color indicator.

The acid number is calculated from this equation:

N= 0.1 (N)

V= volume of NaOH consumed (ml)

W= mass of the sample (g)

The decarboxylation % was calculated using the acid number of oleic acid and acid number of the product using the following relation:

% Decarboxylation= (acid number of oleic acid - acid number of the product) / acid number of oleic acid × 100%

3. Results and Discussion

The SEM images of Cu, Al, and Ga MOFs are shown in Figure 1. Figure 1a shows a representative SEM of Cu-MOF displaying well faceted hexagonal crystals with relatively narrow size distribution and with average particle size in the ~0.8-1 µm range. Figure 1b shows a representative Al-MOF showing hexagonal crystals with a broad size distribution and average particle size in the 0.2~0.8 µm range. Figure 1c shows a representative SEM of Ga-MOF showing larger (~10 µm) dodecahedral crystalline morphology.

Figure 2 shows the XRD patterns of the Cu, Al, and Ga MOFs. Figure 2a shows the XRD pattern of Cu-MOF corresponding to the typical known structure of $Cu_3(BTC)_2$ [41,42]. The metal organic framework, $Cu_3(BTC)_2$ (BTC = benzene-1,3,5-tricarboxylate) is an appealing material to employ as catalyst for the decarboxylation of fatty acid molecules due to the presence of Lewis acid coordination sites (Cu) in its framework. $Cu_3(BTC)_2$ is a porous metal organic framework which forms a face-centered cubic crystalline structure which is composed of dimeric cupric tetracarboxylate units, which give an intersecting 3Dchannel system with micropore diameter of 0.7–0.8 nm [41].Figures 2b and Figure 2c shows the XRD patterns of Al-MOF and Ga-MOF respectively. A shift to lower 2 theta angles in the XRD reflections (as compared to Cu-MOF) for these two samples is evident. This shift suggest a higher degree of local structural disorder which is expected due to the incorporation of larger atoms in the porous framework (Cu atomic radius = 0.127 nm; Ga atomic radius=0.136 nm; Al atomic radius = 0.143 nm) [41]. The XRD patterns of the Pt-supported MOF samples were identical to those of the bare MOFs (not shown here).

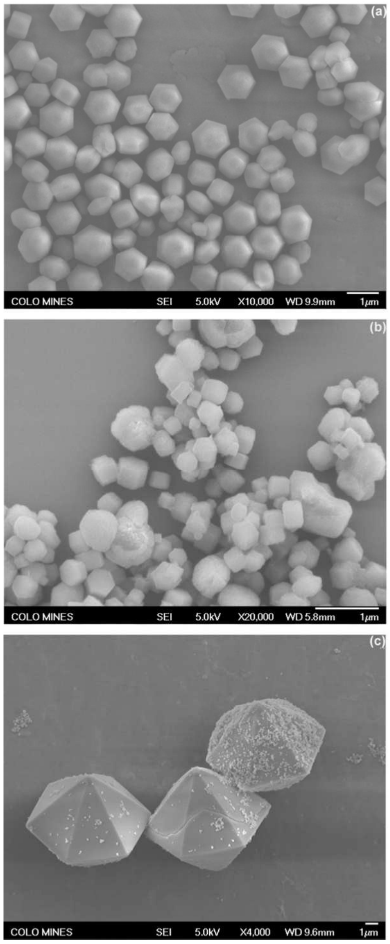

Figure 1. Representative SEM images of (a) Cu-MOF, (b) Al-MOF, and (c) Ga-MOF

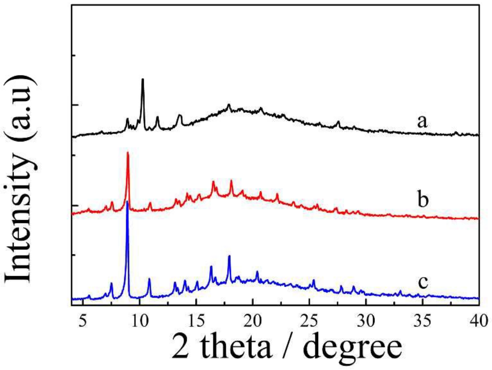

Figure 2. XRD patterns of (a) Cu-MOF, (b) Al-MOF, and (c) Ga-MOF

Figure 3 shows the decarboxylation of oleic acid over Cu-MOF, Al-MOF and Ga-MOF at 320 °C. The degree of decarboxylation increased in the following order: Ga-MOF>AlMOF>CuMOF. More specifically, ~66%, ~45% and ~42% degree of decarboxylation were observed for Ga-MOF, Al-MOF and Cu-MOF respectively. Interestingly the catalytic performance of these isostructural MOFs correlate with the degree of metal acidity. Gallium as hard acid metal is the most acidic, and Cu a borderline acid metal is the less acidic. The observed catalytic activity of these particular MOF compositions (even in the absence of a noble metal) is not surprising since these MOFs have the particular property of exposing their open metal centers making them *chemical reactive.* In addition, we have recently demonstrated that acid supports can help in promoting the decarboxylation of fatty acid molecules such as oleic acid [33]. The presence of H_2 promoted the hydrogenation of oleic acid to stearic acid which then undergoes facile decarboxylation.

Figure 4 shows the decarboxylation of oleic acid over Cu-MOF, Al-MOF and Ga-MOF impregnated with 5 % Pt at reaction temperature of 320°C. As expected, the degree of decarboxylation considerably increased with the addition of Pt. Similar to the catalytic trend observed for the bare MOFs, the following order was observed for the Pt impregnated MOF catalysts: Pt/Ga-MOF>Pt/AlMOF>Pt/CuMOF. In particular, ~92%, ~90% and ~46% degree of decarboxylation were observed for Pt/Ga-MOF, Pt/Al-MOF and Pt/Cu-MOF respectively.

The higher catalytic activity of Pt-based catalysts prepared from the $Pt(NH_3)_4[(NO_3)]_2$ has been reported earlier [3,44,45,33] Cationic complexes (like $Pt[(NH_3)_4]^{2+}$) likely lead to better dispersion and anchoring to the MOF surface and, consequently, to improve catalytic activity.

Recyclability is an important and essential feature of any catalyst to be considered for use in industrial applications. Therefore, we investigated the influence of catalyst recycle on the catalytic performance. Upon recycling the catalysts (Figure 4), slightly lower decarboxylation % were observed. This relatively low loss in catalytic activity for the recycled catalysts can be explained in part by the remarkable thermal stability of Cu-MOF, Al-MOF and Ga-MOF crystals. As shown in Figure 5, all samples were thermally stable at least up to ~330°C. More specifically, Cu-MOF displayed ~10% weight loss at ~ 330 °C; Al-MOF displayed ~15% weight loss at ~ 520 °C and Ga-MOF displayed ~15% weight loss at ~ 500 °C .

We performed EDX analysis, and no significant changes in metal content were observed for Ga-MOF based samples, suggesting that there is no metal leaching. For example for Pt-GaMOF before reaction (% wt Pt 4.3±0.8) after reaction (% wt Pt 4.1±0.6). For GaMOF before reaction (% wt Ga 56.5±0.5) after reaction (% wt Ga 55.8±0.9).

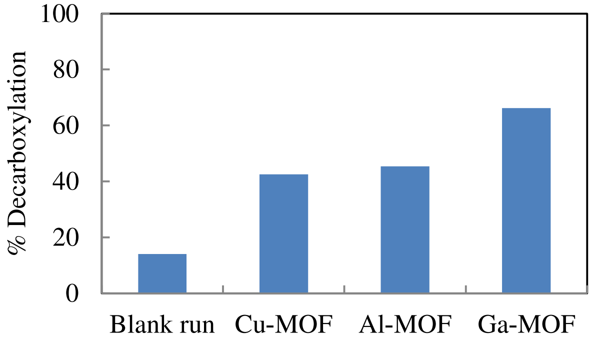

Figure 3. Decarboxylation of oleic acid over Cu-MOF, Al-MOF, Ga-MOF catalysts and blank run (Reaction conditions: 10 ml oleic acid, 0.5 g catalyst, 2 hr, and pressure 20 bar at 320°C)

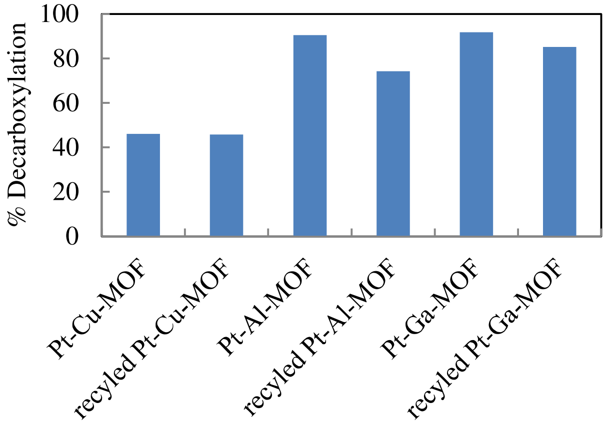

Figure 4. Decarboxylation of oleic acid over fresh and *recycled* Pt/Cu-MOF, Pt/Al-MOF and Pt/Ga-MOF catalysts

(Reaction conditions: 10 ml oleic acid, 0.5 g catalyst, 2 hr, and pressure 20 bar at 320°C).

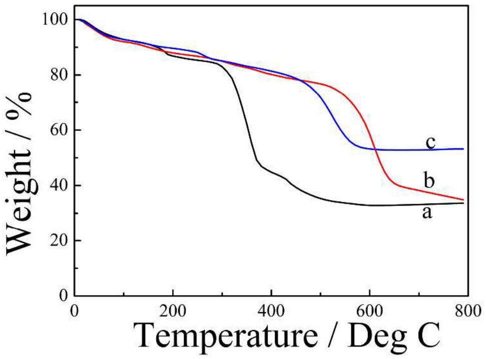

Figure 5. TGA profiles of (a) Cu-MOF, (b) Al-MOF, and (c) Ga-MOF

The detailed product distribution for the most active catalysts (Ga-MOFs with and without Pt) is given in Table 1. The components in the liquid product included branched paraffins formed by isomerization of the initially formed heptadecane, and lower molecular weight hydrocarbons (mostly C_7-C_{18} paraffins) formed by cracking of the heptadecane. No oleic acid was observed in the products under all reaction conditions, suggesting total conversion of oleic acid. Octadecane, heptadecane, dodecane, undecane, decane, nonane, octane, heptane were observed as the main side products.

As shown in Figure 6, under similar reaction conditions (temperature, pressure, reaction time), the selectivity to heptadecane over Pt/Ga-MOF was comparable to other Pt supported porous crystalline supports, such as zeolite RHO and hydrotalcite, but lower than supports such as zeolites DNL-6 and SAPO-34 [33]. The lower selectivity may be related to a *restricted transition state selectivity* [46] observed in small pore zeolites like SAPO-34 and DNL-6. More specifically, on supported metal, bifunctional catalysts, like those used in the present and in our previous report [33], the selectivity for the initially formed linear paraffin, heptadecane (amongst the reaction products) is inversely proportional to the ability of the catalyst to isomerize it , further to branched paraffins over the acidic sites of the support. In addition to the acidity, the pore diameter of the support also plays a crucial role: Supports with smaller pore diameters (like SAPO-34 and DNL-6) prevent the further isomerization reaction of heptadecane since the large size of the transition state needed for the isomerization cannot be accomodated in the constrained confines of the small pores (restricted transition state selectivity [46]. In restricted transition state-type selectivity, certain reactions (like the isomerization of linear to branched olefins / paraffins are prevented because the transition state is too large for the cavities of the catalyst. SAPO-34 belongs, structurally, to the chabazite group of zeolites. It contains 8-membered ring pores with openings of 0.38 nm. DNL-6 is structurally related to zeolite Rho with pore size of 0.36 nm (close to SAPO-34). Interestingly, both supports with very close pore size show the highest selectivity to heptadecane, suggesting "molecular sieving" effect. On the other hand, the other supports showing lower heptadecane selectivity have larger or smaller pore sizes. For instance, Ga-MOF (isostructural form of Cu-MOF) has pore size, of ~0.8 nm. Hydrotalcite also has larger pore size. Zeolite RHO has a pore system comprising of 8-membered rings with pore openings that can be as small as 0.29 nm. In the case of RHO, the smaller pore size may impose diffusion limitations, resulting in low heptadecaneselectivities.

Therefore, the isomerization of heptadecane to bulkier branched isomers will, hence, be sterically more difficult, relatively, in the narrow pores of SAPO- 34 or DNL-6 than in the other supports having larger or smaller pore sizes (like Ga-MOF, hydrotalcite, and zeolite RHO), accounting for its higher selectivity for the linear heptadecane.

Typical heptadecane yield for Pt carbon supported catalysts (at comparable reaction conditions) is ~15% [32]. Although for Pt/Ga-MOF, this yield is ~ 20%, yields as high as ~64% has been observed for Pt/SAPO-34 catalysts [33].

Not only pore size, but also chemical composition, acidity of the support (surface functionality), and dispersion of the Pt are other key factors in controlling the catalytic activity and product selectivity in the conversion of oleic acid to hydrocarbons.

Currently, we are exploring the use of MOFs with pore sizes that in principle may lead to the molecular sieving effect observed in DNL-6 and SAPO-34. These MOF compositions include ZIF-8 and ZIF-67 which have limiting pore apertures of 0.34 nm.

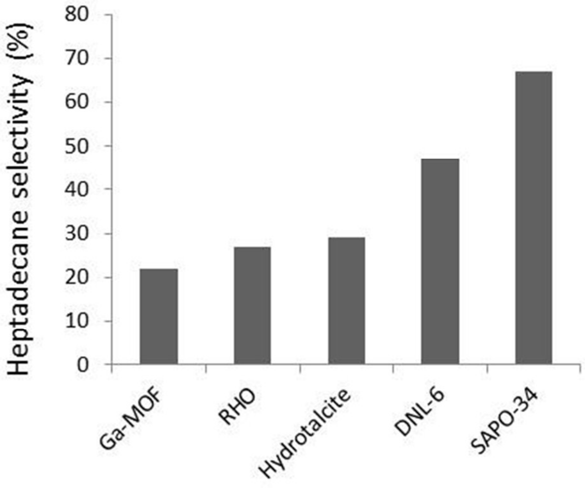

Figure 6. Heptadecane selectivity for several Pt supported catalysts.(Reaction conditions: 10 ml oleic acid, 0.5 g catalyst, 2 hr, and pressure 20 bar at 325°C. Only for Ga-MOF temperature was 320 °C).

The general decarboxylation reaction scheme of the conversion of oleic acid to hydrocarbons over MOF catalysts is shown in Fig. 7 .

.

Table 1. Liquid product distribution for the decarboxylation of oleic acid over Pt/Ga-MOF and Ga-MOF catalysts

Reaction conditions				Hydrocarbon products (%)								
Catalyst	Pressure (bar)	Temperature (°C)	Time (h)	Octadecane	Heptadecane	Dodecane	Undecane	Decane	Nonane	Octane	Heptane	Gas [a]
5% Pt-Ga-MOF	20	320	2	55.13	21.52	-	0.92	1.46	1.71	1.81	1.53	15.92
Ga-MOF	20	320	2	-	5.70	6.72	9.19	9.32	12.76	15.84	12.82	27.65

[a] Mass balance (CO_2, CH_4, others)

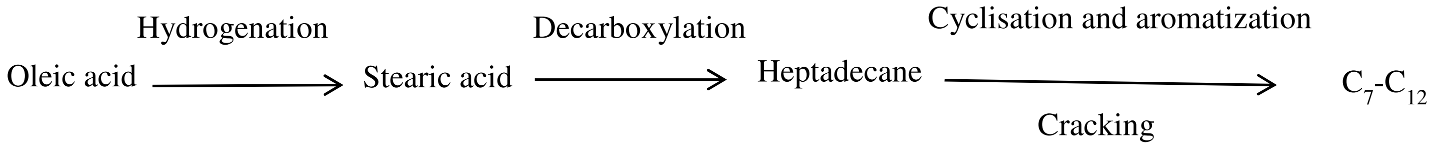

Figure 7. Scheme showing the general pathway of the reaction

4. Conclusions

The decarboxylation and further conversion of oleic acid to gasoline/diesel-range hydrocarbons has been demonstrated over bare and Pt supported Cu, Al and Ga based metal organic frameworks. Moderate degree of decarboxylation (42-66%) were observed for all metal organic framework catalysts. The incorporation of Pt with the porous frameworks resulted in high degrees of decarboxylation (above 90% for Al-MOF and Ga-MOF). All MOF catalysts displayed high thermal stability, resulting in recyclable catalysts displaying low catalytic activity loss. In particular, Ga-MOF catalysts were the most effective catalysts, displaying moderate to high degrees of decarboxylation. The improved catalytic performance of Ga-MOF may be related with the higher acidity of Ga. In addition, the Pt-Ga-MOF catalyst displayed selectivity to heptadecane, an important industrial chemical. Octadecane, heptadecane, dodecane, undecane, decane, nonane, octane, heptane were observed as the main side products. To our best knowledge, the catalytic ability of a metal organic framework both as catalyst and support for the decarboxylation of a model fatty acid molecule is demonstrated for the first time.

Notes:

Chemical and Biological Engineering Department, Colorado School of Mines, Golden CO 80401

* Corresponding author (mcarreon@mines.edu)

Acknowledgements

We thank Coors foundation for financial support of this work.

References

[1] J. Fu, X. Lu, P. E. Savage, L. T. Thompson, Jr. Xiuyang Lu, *American Chemical Society Catalysis*. 2011, **1**, 227–231.

[2] P. Arvela, B. Rozmysłowicz, S. Lestari, O Simakova, K. Eränen, T. Salmi, D.Yu. Murzin, *Energy Fuels*, 2011, **25**, 2815–2825.

[3]E. Laurent, B. Delmon, *Appllied Catalysis A: General*. 1994, **109**, 77-96.

[4] M. Snåre, I. Kubickova, P.Arvela, K. Eranen, D. Yu. Murzin, *Industerial and Engineering Chemistry Research,* 2006, **45**, 5708-5715.

[5] M. Snare, I. Kubickova, P. Maki-Arvela, D. Chichova, K. Eranen, D.Yu. Murzin, *Fuel*.2008, **87**, 933–945.

[6] R. Stern, G. Hillion.; *US Pat*.1985, **4**, 695,411.

[7] G.W. Huber, A. Corma, Angew. *Angewandte Chemie International Edition*., 2007, **46**, 7184–7201.

[8] S. Lestari, P. Maki-Arvela, K. Eranen, J. Beltramini, G.Q. Max Lu, D.Y. Murzin, *Catalysis Letter*. 2010, **134**, 250–257.

[9] H. Bernas, K. Eranen, I. Srimakova, A.R. Leino, K. Kordas, J. Myllyoja, P. Maki-Arvela, T. Salmi, D.Y. Murzin, *Fuel.* 2010, **89**, 2033–2039.

[10] M. Snåre, I. Kubickova, P.Arvela, K. Eranen, D. Yu. Murzin, *Catalysis Today*, 2005, **106** 197–200.

[11] M. Snåre, I. Kubickova, P.Arvela, K. Eranen, D. Yu. Murzin,*Catal Org React*, 2006, **115**, 415–425.

[12] D. Yu. Murzin, I. Kubickova, M. Snåre, P.Arvela, *European Patent Application*. 2005, 05075068.6.

[13] A. Sivasamy, K. Cheah, P. Fornasiero, F. Kemausuor, S. Zinoviev, S. Miertus, *Chemistry & Sustainability, energy & materials (ChemSusChem.),* 2009, **2**, 278 – 300.

[14] H L. Ngo, N A. Zafiropoulos, T A. Foglia, E T. Samulski, W. Lin, *Energy & Fuels*, 2008, 22, 626-634.

[15] M J. Haas, A J. McAloon, W C. Yee, T A. Foglia, *Bioresource Technology*, 2006, **97**, 671-678.

[16] B. Renard, J R. Jr, D. Duprez, S. Durécu, *Applied Catalysis B: Environmental*, 2005, **55**, 1-10.

[17] F.A. Twaiq, N.A.M Zabidi, S.Bhatia, *Industerial and Engineering Chemistry Research,* 1999, **38**, 3230–3237.

[18] WK. Craig, DW. Soveran, *US Pat*.1991, 4,992,605.

[19] D. Lima, VC. Soares, EB. Ribeiro, DA. Caravalho, ECV. Cardoso, FC. Rassi, et al. *Journal of Analytical and Applied Pyrolysis*, 2004, **71,** 987–996.

[20] M. Arenda, T. Nonnena, W. F. Hoeldericha, J. Fischerb, J. Groosb, *Applied Catalysis A*: *General*. 2011, **399**, 198–204.

[21] DR. Vardon, BK. Sharma, H. Haramillo, D. Kim, JK. Choe, PN. Ciesielski ,TJ. Strathmann.*Green Chem.,* 2014, **16**, 1507-1520.

[22] JP. Ford, N. Thapaliya, MJ. Kelly, WL. Roberts , HH. Lamb.*Energy Fuels*, 2013, **27**, 7489-7496.

[23] JG. Immer, MJ. Kelly, HH. Lamb.*Applied Catalysis A: General* ,2010,375, 134-139.

[24] J.Monnier, H. Sulimma, A. Dalai ,Gianni Caravaggio. *Applied Catalysis A: General* ,2010, **382**, 176-180.

[25] JG. Na, BE. Yi, JK. Han, YK. Oh, JH. Park, TS. Jung, SS. Han, HC. Yoon, JN. Kim, H. Lee and CH.Ko.*Energy*2012,**47**, 25-30.

[26] JG. Na, BE. Yi, JN. Kim, KB. Yi, SY. Park, JH. Park, JN. Kim ,CH.Ko. *Catalysis Today* 2010,**156**, 44-48.

[27] HS.Roh, IH.Eum, DW.Jeong, BE. Yi, JG. Na and CH. Ko. *Catalysis Today* 2011,**164**, 457-460.

[28] LRR. Araujo, CF.Scofield, NMR.Pastura and WA. Gonzalez.*Materials Research*, 2006, **9**, 181-184.

[29] B. Levasseur, B. Renard, J. Barbier, Jr. ,D. Duprez, *React. Kinet.Catal.Lett., ,*2006**,** **87**, 269-279.

[30] AG. Gasanov, AG. Azizov, SR. Khalilova, IG. Ayubov, MM. Gurbanova ,ST. Alieva. *Russian Journal of Applied Chemistry*, 2014, **87**, 214-216.

[31] R E. Murray, E L. Walter, K M. Doll, *ACS Catal*., 2014, 4, 3517-3520.

[32] M. Ahmadi, E. E. Macias, J.B. Jasinski, P. Ratnasamy, M.A. Carreon, *Journal of Molecular Catalysis A: Chemical ,* 2014, **386**, 14–19.

[33] M. Ahmadi, A. Nambo, J. B. Jasinski, P. Ratnasamy and M. A. Carreon, *Catal.Sci.Technol.* 2015, **5**, 380-388.

[34] KS. Park, Z. Ni, AP. Côté, JY. Choi, R. Huang, FJ. Uribe-Romo, HK.Chae, M.O'Keeffe, OM. Yaghi, *Proc. Natl. Acad. Sci. U. S. A*. 2006,**103**, 10186–10191.

[35] OM.Yaghi, M. O'Keeffe, NW. Ockwig, HK.Chae, M. Eddaoudi, J.Kim. *Nature* 2003,**423**, 705–714.

[36] G. Férey. *Chem. Soc. Rev.*2008, **37**, 191–214.

[37] L.MacGillivray. Metal Organic Framework: Design and Application .John Wiley & Sons. (2010).

[38] D. Farrusseng, S. Aguado, *Angew. Chem. Int. Ed*. 2009,**48**, 7502-7513.

[39] D. Farrusseng, Metal organic frameworks: Applications from Catalysis to gas storage, Wiley-VCH (2011)

[40] K. Lin, A K. Adhikari, C. Ku, C. Chiang. H. Kuo, *International Journal of Hydrogen Energy*, 2012, 37, 13865-13871.

[41] K. Schlichte, T. Kratzke, S. Kaskel. *Microporous Mesoporous Materials*, 2004, **73**, 81-88.

[42]L. Alaerts, E. Seguin, H. Poelman, F. Thibault-Starzyk, PA.Jacobs, DE. De Vos. *Chemistry: A European Journal*, 2006, **12**, 7353-7363.

[43] Jr. WD. Callister, DG. Rethwisch. Fundamentals of Materials Science and Engineering. An integrated approach.John Wiley & Sons. (2012).

[44] S. H. Bertram, *Chemisch. Weekblad*. 1936, **33**, 457-459.

[45] A.T Madsen, E. Ahmed, C. H. Christensen, R. Fehrmann, A. Riisager, *Fuel*, 2011**, 90**, 3433–3438.

[46] Sigmund M. Csicsery, *Pure & Applied Chemistry*, 1986**, 58**, 841-856.